

A multichannel native fluorescence detection system for capillary electrophoretic analysis of neurotransmitters in single neurons

T. Lapainis · C. Scanlan · S. S. Rubakhin · J. V. Sweedler

Received: 21 June 2006 / Revised: 8 August 2006 / Accepted: 10 August 2006
© Springer-Verlag 2006

Abstract A laser-induced native fluorescence detection system optimized for analysis of indolamines and catecholamines by capillary electrophoresis is described. A hollow-cathode metal vapor laser emitting at 224 nm is used for fluorescence excitation, and the emitted fluorescence is spectrally distributed by a series of dichroic beam-splitters into three wavelength channels: 250–310 nm, 310–400 nm, and >400 nm. A separate photomultiplier tube is used for detection of the fluorescence in each of the three wavelength ranges. The instrument provides more information than a single-channel system, without the complexity associated with a spectrograph/charge-coupled device-based detector. With this instrument, analytes can be separated and identified not only on the basis of their electrophoretic migration time but also on the basis of their multichannel signature, which consists of the ratios of relative fluorescence intensities detected in each wavelength channel. The 224-nm excitation channel resulted in a detection limit of 40 nmol L⁻¹ for dopamine. The utility of this instrument for single-cell analysis was demonstrated by the detection and identification of the neurotransmitters in serotonergic LPeD1 and dopaminergic RPeD1 neurons, isolated from the central nervous system of the well-established neurobiological model *Lymnaea stagnalis*. Not only can this system detect neurotransmitters in these individual neurons with $S/N > 50$, but analyte identity is confirmed on the basis of spectral characteristics.

Keywords Capillary electrophoresis · Laser-induced native fluorescence detection · Single-cell analysis · Dopamine · *Lymnaea stagnalis*

Abbreviations

5-HT	serotonin
ASW	artificial sea water
CE	capillary electrophoresis
CNS	central nervous system
CW	continuous wavelength
DA	dopamine
EC	electrochemical detection
LINF	laser-induced native fluorescence
MCC	metacerebral cells
PMT	photomultiplier tube
Trp	tryptophan
Tyr	tyrosine
OA	octopamine

Introduction

The development of analytical techniques capable of probing the chemical composition of individual cells is important for accelerating progress in the bioanalytical and clinical sciences. For example, the diversity in function and the biochemical complexity of the different neurons present in every neuronal circuit requires analytical techniques capable of probing cell-to-cell signaling molecules in individual neurons and even subcellular domains. Of interest is the cellular and subcellular distribution of catecholamines and indolamines, for example serotonin (5-HT) and dopamine (DA). These intercellular signaling molecules are known for their involvement in a variety of

Lapainis and Scanlan contributed equally to this work.

T. Lapainis · C. Scanlan · S. S. Rubakhin · J. V. Sweedler (✉)
Department of Chemistry and the Beckman Institute,
University of Illinois, 600 S. Matthews Ave., Box 63-5,
Urbana, IL 61801, USA
e-mail: sweedler@scs.uiuc.edu

mechanisms in a normally functioning nervous system, and in different pathological manifestations. In addition to these well-studied neurotransmitters, there is interest in probing the distribution of a variety of other biogenic amines, for example octopamine (OA) and tyramine [1, 2].

Capillary electrophoresis (CE) is an analytical technique that is particularly well-suited to performing cellular and subcellular analysis [3–6]; the separation efficiency of CE is high, yet it requires relatively small sample volumes—femtoliter to picoliter—compatible with single-cell measurements [7]. For single-cell analysis, intact cells can be hydrodynamically or electrokinetically injected into the capillary, followed by on-capillary lysis and separation [8, 9]. For subcellular analysis, a microinjector can be fashioned and used to probe the cytoplasm of a cell, leaving the cell intact while interrogating the subcellular contents [10], or different regions of a cell can be separately collected and analyzed [11].

A variety of detection schemes have been used in conjunction with CE, including electrochemical (EC) [12], laser-induced fluorescence (LIF) [13, 14], and mass spectrometric (MS) [15] detection. EC detection is advantageous when the analyte of interest is electroactive, nonfluorescent, and/or cannot be suitably derivatized with a fluorophore [8]. CE-LIF can be performed with detection of native fluorescence (LINF) [14, 16–19], multiphoton native fluorescence [20, 21], or fluorescence after derivatization with a fluorophore [13, 22–25]. Derivatization usually results in high sensitivity, but non-specific and incomplete derivatization may limit application of this method; the latter is especially significant in single-cell and subcellular analysis, given the small volumes of samples and the amounts of materials being analyzed.

CE-LINF was originally performed using a single-channel photomultiplier-based (PMT) detection system. Yeung and Chang [14] focused the 275-nm line of an Ar⁺ laser to a spot through a detection window on the capillary and used a PMT to detect the resulting fluorescence signal. They obtained limits of detection (LOD) as low as 30 nmol L⁻¹ for DA. Timperman and Sweedler [17, 19] developed a wavelength-resolved CE-LINF instrument to supplement the information content of the electropherogram by providing the fluorescence emission spectrum of each eluting analyte. In that system, a frequency-doubled Ar⁺ or Kr⁺ laser was focused immediately below the outlet of the capillary, which was housed in a sheath-flow cuvette. Use of such a cuvette reduces signal losses resulting from scattering from the curved surface of the capillary and minimizes background fluorescence associated with metal ions within the fused silica capillary [13, 17, 24, 26]. With our previous system the fluorescence was collected with a microscope objective, wavelength-resolved via a spectrograph, and projected on to a charge-coupled device (CCD)

[27]. Not only does this instrument have excellent LODs for indolamines such as 5-HT, it can also be used to distinguish between different species with nearly identical migration times on the basis of their fluorescence spectra [4]. The spectral information can also compensate for the inconsistency of migration times that results from injecting cellular debris into the capillary.

Here we describe a CE-LIF system that exploits the relative simplicity and sensitivity of PMT-based detection and the enhanced spectral information associated with a spectrograph/CCD-based detector. To do this, we used a series of dichroic beam-splitters to split the fluorescence signal on the basis of emission wavelength and to transmit each wavelength range to one of three PMTs. A pulsed 224-nm HeAg metal vapor laser was used for excitation; this system has lower power consumption than the more commonly used full-frame ion lasers [11, 28]. We have previously characterized longer-wavelength metal-vapor lasers for CE [11, 28] but selected the 224 nm HeAg because of its capacity to excite a broad range of neuroactive compounds. Custom PMT controller boards interface directly to the pulsed laser, enabling fluorophore excitation and fluorescence detection to be synchronized, thus minimizing the detection of background between laser pulses. The instrumentation is simple to operate and maintains information content higher than typical single-channel detection systems. It is, furthermore, less expensive than other ultraviolet (UV) LINF systems. This reduction in cost is significant, given that cost seems to be a primary hindrance to widespread use of LINF as a detection method. To characterize the ability of the system to perform single-cell catecholamine and indolamine analysis, we assayed single identified neurons (LPeD1 and RPeD1) from the central nervous system (CNS) of the pond snail *Lymnaea stagnalis*, and confirmed analyte identity by use of spectral characteristics.

Experimental

Materials

Citric acid sheath buffer (25 mmol L⁻¹, pH 2.5) was prepared by dissolving 5.25 g citric acid monohydrate (C₆H₈O₇·H₂O; Sigma, St Louis, MO, USA) in 1.0 L ultrapure deionized water (Elga Purelab Ultra water system; USFilter, Lowell, MA, USA) and titrating to pH 2.5 with 0.10 mol L⁻¹ NaOH. Citrate running buffer (25 mmol L⁻¹, pH 5.5) was made from the same stock, but was titrated to pH 5.5 with 1.0 mol L⁻¹ NaOH. The buffers were then filtered with a 0.45 μm bottle-top filter system (Nalgene, Rochester, NY, USA) and degassed under vacuum with stirring for ~1 h. All standards were obtained from Sigma

optics with an MgF₂-coated, all-reflective microscope objective (13596, Newport, Irvine, CA, USA) with a 0.4 numerical aperture. The laser line was spectrally filtered by means of a 250-nm long-pass filter (Barr Associates, Westford, MA, USA); fluorescence was then transmitted or reflected by one or both custom dichroic beam-splitters (Model and lot numbers 310dcxxr-haf #110258 and 400dcxru #111563, Chroma Technology, Rockingham, VT, USA). The beam-splitters had transition points at 310 nm and 400 nm, respectively. Spectrally distributed fluorescence was detected by one of three PMTs (H6780-06; Hamamatsu, Middlesex, NJ, USA), and the three channels corresponded to wavelength ranges of 250–310 nm, 310–400 nm, and >400 nm.

The PMTs were connected to individual controller boards (Rev. C, Photon Systems) that were plugged into the laser, which in turn was connected to a personal computer (Dimension 8200; Dell, Round Rock, TX, USA) via a USB 2.0 cable. Because the controller boards interfaced directly to the laser, the integration time of the PMTs could be precisely synchronized with the laser pulse. Board settings, for example PMT control voltage, were optimized independent of each of the other boards, enhancing flexibility in detection optimization. In addition, each board had an array of capacitors that were used for additional control over the PMT gain. Control software, written in LabVIEW (National Instruments, Austin, TX, USA) and provided by Photon Systems, controlled the laser and the PMTs. Thus, the settings of the controller boards (and the laser) could be modified in real-time during sample analysis, extending the effective dynamic range of the instrument.

The fluorescence emission spectra were obtained using the previously described wavelength-resolved CE-LINF arrangement [17] except the laser was changed to the Photon Systems HeAg 70 laser for 224 nm excitation. Briefly, a syringe pump (Sage M361, Orion, Waltham, MA, USA) was used to maintain a constant stream (0.26 mL h⁻¹) of analyte at the outlet of the capillary. Fluorescence emission was collected using an all-reflective microscope objective (same as above), and focused on to a spectrograph (CP140, J. Y. Horiba, Edison, NJ, USA). The wavelength-resolved fluorescence was then detected using a liquid nitrogen-cooled CCD (Photometrics, Tucson, AZ, USA).

Electrophoresis

For all experiments, the sheath-flow solution was 25 mmol L⁻¹ citrate buffer (pH 2.5), and the running buffer was 25 mmol L⁻¹ citrate (pH 5.5). Separations were performed at +24.3 kV, which corresponded to a current of ~30 μA. Standard solutions were prepared in 2.5 mmol L⁻¹ citrate buffer (pH~2.5), and ~7.5 nL of the solution was injected

hydrodynamically into a 100-cm-long capillary by lowering the outlet 15 cm below the inlet for 30 s. For whole-cell sample injections the capillary length was reduced to ~70 cm. Immediately after isolation the cell was suspended in ~300 nL of 2.5 mmol L⁻¹ citrate buffer (pH 2.5) on the flat top of a custom-made stainless steel injection pedestal. A stereomicroscope was used to observe the injection apparatus. The pedestal was placed directly under the capillary inlet, which was then lowered into the buffer droplet containing the cell. Next, the outlet of the system was lowered until most of the buffer droplet and the cell were loaded into the capillary. Finally, the inlet was placed into the buffer reservoir, and separation and detection were performed as described above. It was noted that the separation current was lower in experiments in which cellular samples were analyzed, e.g. ~25 μA compared with ~30 μA for solutions containing standards.

Limits of detection

To calculate limits of detection (LOD) for DA, standard curves were generated using several different concentrations of DA, ranging from 5 μmol L⁻¹ to within a factor of two of the initial LOD calculated using the unsmoothed data. The raw data were six-point boxcar averaged [29]. Fluorescence intensity values were normalized such that the baseline corresponded to an intensity value of zero arbitrary fluorescence units. The standard deviation was calculated for a length of baseline approximately equal to the peak width, and the values were averaged for all runs used to construct the standard curve. The criterion used to determine the LOD was three times the average standard deviation of the baseline. When appropriate, linear models were forced through zero. LODs for the other reported catecholamines were calculated in an analogous fashion.

Results and discussion

System design and characterization

A schematic diagram of the multichannel CE-LINF system is given in Fig. 1. The instrument uses a hollow-cathode HeAg laser emitting at 224 nm as the excitation source. This 224-nm radiation excites the S₀→S₂ transition of catecholamines, which has a larger cross-section than the S₀→S₁ transition excited by the 257, 275, or 287-nm radiation generated by other commonly used UV lasers [30]. This results in more intense fluorescence per unit of input power for catecholamines such as DA and OA, while maintaining efficient excitation of indolamines and the aromatic amino acids. Emission spectra of different fluorophores of interest, excited using the 224-nm HeAg

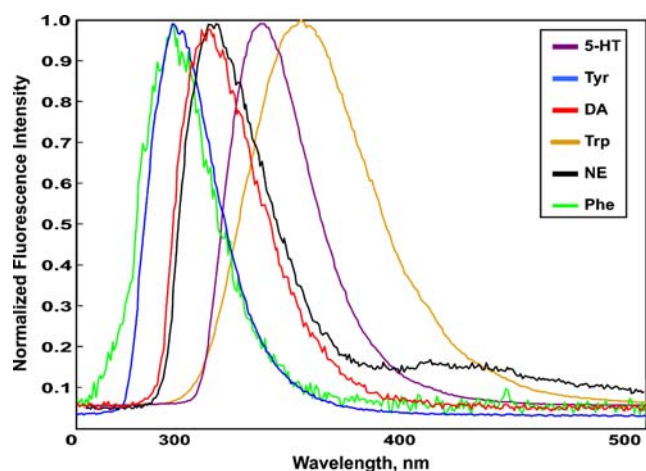
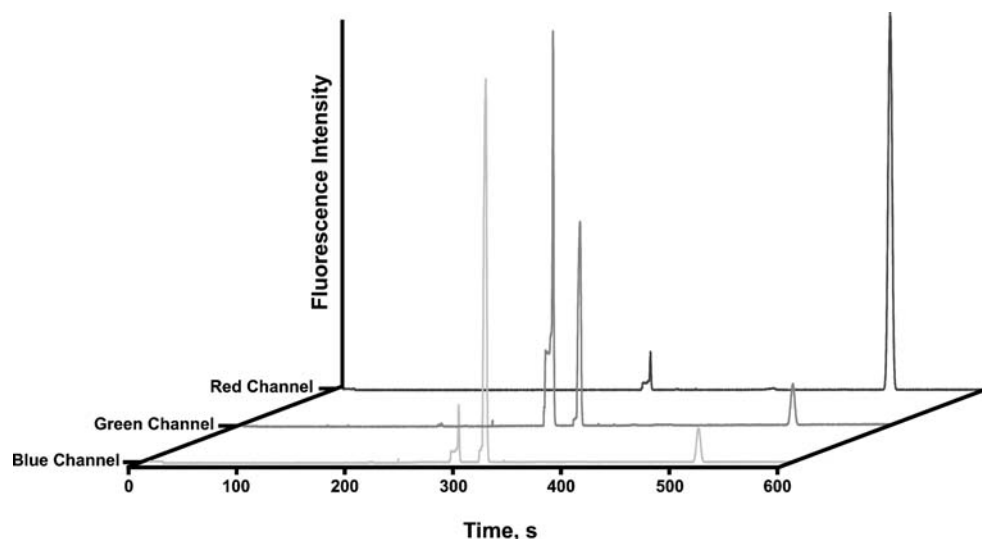


Fig. 2 Emission spectra obtained from six standards, using 224 nm excitation, generated using the previously described wavelength-resolved CE-LIF system [17]. For clarity, standards are listed in order of increasing fluorescence emission λ_{max} . The spectra were used to determine suitable transition wavelengths for the dichroic beam-splitters

laser, are shown in Fig. 2. This information was used to determine suitable transition wavelengths for the dichroic mirrors used in the multichannel detection system. These bands were chosen to optimize the discrimination among the background, the catecholamines, and the indolamines. The wavelengths were 310 nm and 400 nm. The collection optics included a 250-nm long-pass filter, so that the three detection channels corresponded to nominal wavelength ranges of 250–310 nm, 310–400 nm, and >400 nm. Representative three-channel electropherograms are shown in Fig. 3. Tyrosine and the catecholamines emit primarily in the two shorter-wavelength ranges (the “blue” and “green” channels) whereas tryptophan and related indolamines yield an additional signal above 400 nm (the “red” channel).

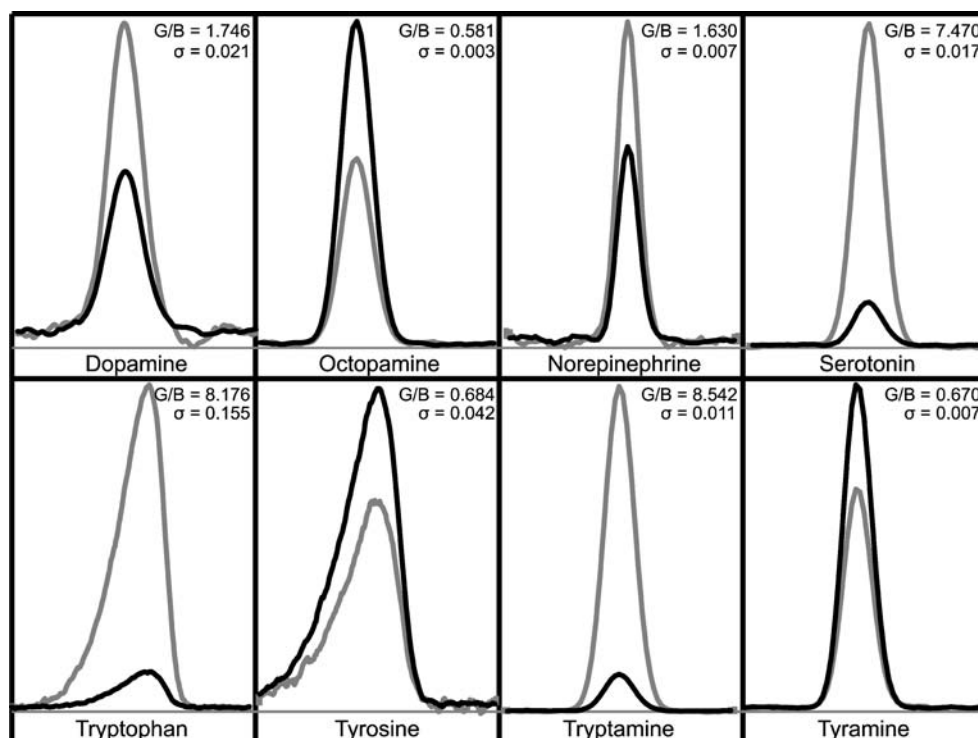
Fig. 3 Separation of Trp, Tyr, and FITC with the CE-LINF multichannel detection system. Tyr is collected primarily in the “Blue” channel (250–310 nm), Trp in the “Green” channel (310–400 nm), and FITC in the “Red” channel (400+nm)



In addition to its use for characterizing tryptophan-based fluorophores, the red channel can also serve several other functions. For example, because many catecholamines can be identified on the basis of their emission in the green and blue channels (see below) an internal standard that co-elutes with other analytes in the separation but emits primarily in the red channel can be used without substantially hindering the identification process; this makes selection of an appropriate internal standard easier. Also, because most common derivatization agents emit above 400 nm, LIF of labeled analytes can be detected in the red channel, taking advantage of the ability of the sheath-flow cuvette to serve as an online derivatization reactor [24].

It is important that the increased information content provided by multiple detection channels is not accompanied by a corresponding loss in detectability. Not only are LODs for catecholamines improved compared with the CCD-based LINF system (using 257-nm excitation), they are similar to those of previous single-channel CE-LINF systems. The LOD for DA is 40 nmol L⁻¹ compared with 120 nmol L⁻¹ for the CCD-based system [29] and comparable with the lowest LOD reported for a single-channel PMT-based system (30 nmol L⁻¹ [14]). LODs for two other catecholamines measured with this system, norepinephrine (NE, 44 nmol L⁻¹) and octopamine (OA, 11 nmol L⁻¹), are also improved [29]; these improvements are partly because of the choice of excitation wavelength. The system also enables sensitive detection of indolamines; the LOD for serotonin is of the order of 10 nmol L⁻¹, comparable with that of the CCD-based detection system (6 nmol L⁻¹) [29]. Although the “blue” and “green” channels yielded similar LODs, the “blue” channel usually gave the lowest LODs. The difference between calculated LOD for these channels was greatest for octopamine, for which LOD_{Blue}=6 nmol L⁻¹ and LOD_{Green}=26 nmol L⁻¹ for the same data set.

Fig. 4 Fluorescence intensity ratios between the green (310–400 nm) and blue (250–310 nm) channels (S_G/S_B), and associated errors (σ =standard deviation), for eight standards detected by use of the multichannel system



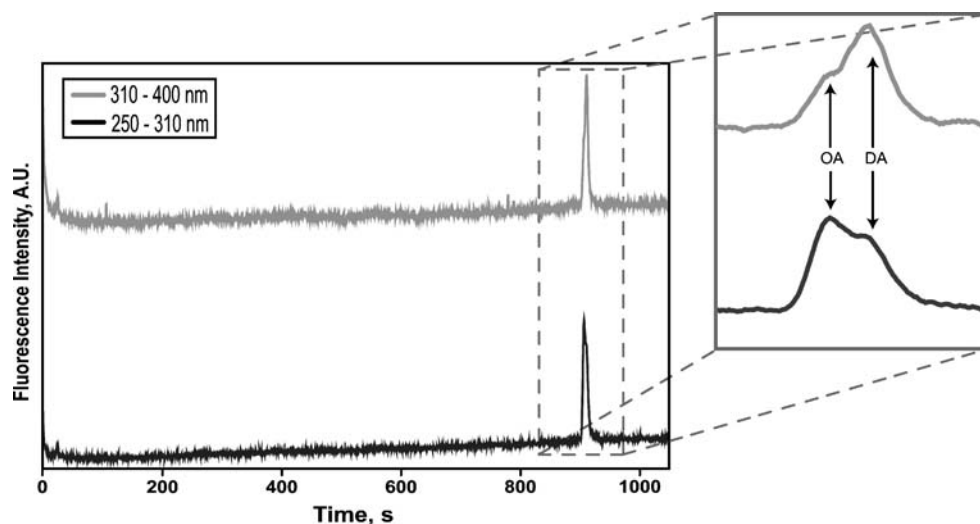
Spectral differentiation of analytes

In CE, identification of an analyte is primarily based on migration time. As mentioned above, confirmation of analyte identity can be aided by monitoring the relative emission in the blue and green channels. To do this, the ratio $S_{\text{green}}/S_{\text{blue}}$ is calculated, where S is the peak intensity minus the average baseline value immediately preceding the peak. Figure 4 shows the relative peak heights and ratios for several neurotransmitters. Although some analytes (e.g. tyrosine and tyramine) yield similar signals, differences between their electrophoretic mobility provide

confirmation of peak identity ($t_m \sim 1300$ s for tyrosine and ~ 615 s for tyramine). In addition, the signal from the red channel (not shown) often provides a qualitative means of differentiating such analytes.

The ability to confirm the identity of an analyte aided by its spectral characteristics is particularly advantageous for mass-limited or volume-limited samples, because it eliminates the need to spike a sample with the tentatively identified substance. In whole-cell injections, spiking experiments are problematic, because the entire sample is used during analysis. The use of ratiometry also aids interpretation of electropherograms of complex samples,

Fig. 5 Capability of the multi-channel system to distinguish between two components of an unresolved mixture on the basis of different spectral characteristics. The components of this standard mixture were DA ($2.5 \mu\text{mol L}^{-1}$) and OA ($0.5 \mu\text{mol L}^{-1}$)



because reproducible migration times are less critical. This, too, is advantageous for whole-cell analysis and other volume-limited samples that cannot be filtered, because cellular debris interferes with electroosmotic flow and thus reduces migration time reproducibility.

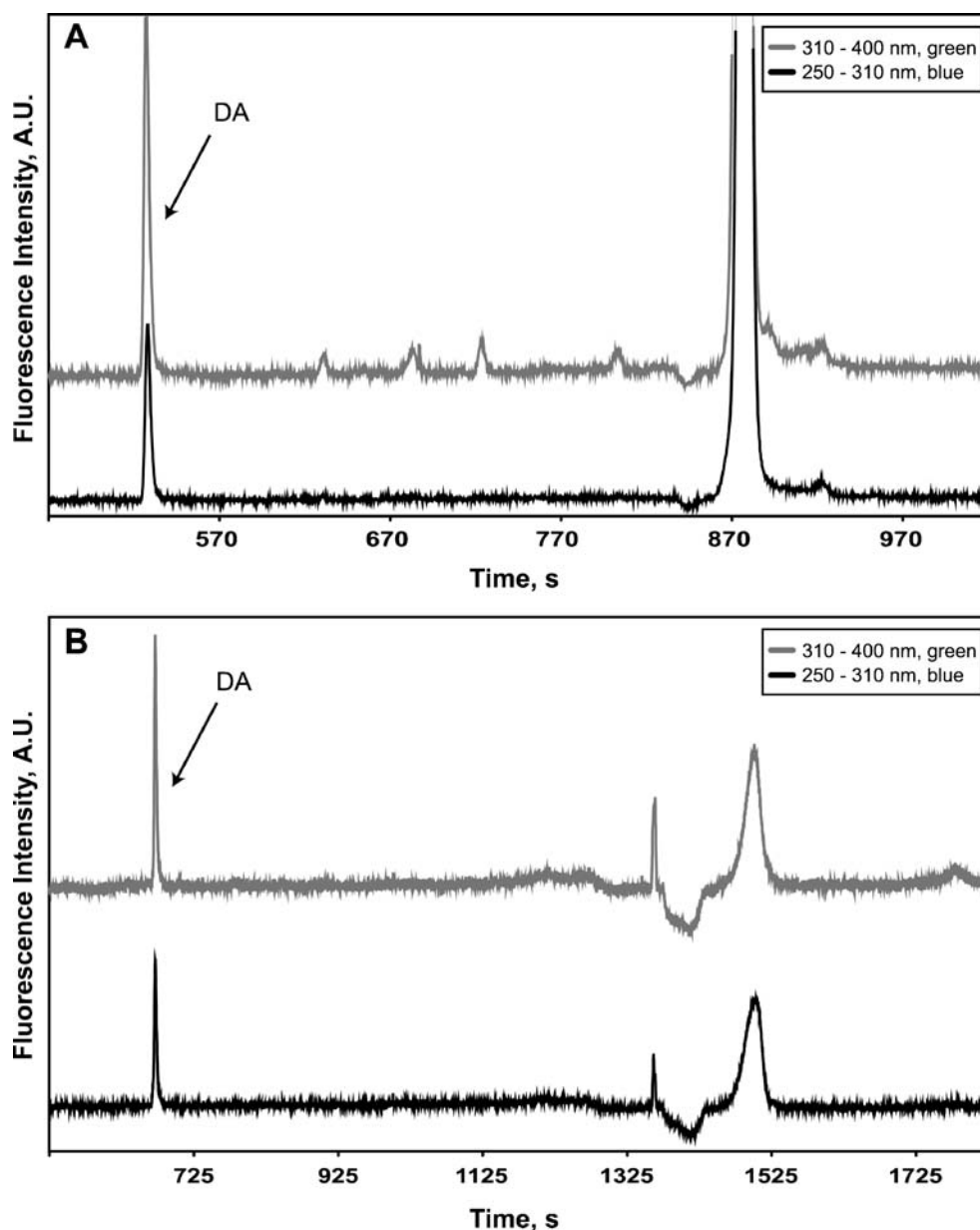
The use of multichannel detection also enables confirmation of peak purity, similar to UV-visible absorbance. An example is presented in Fig. 5, which shows an unresolved mixture of OA and DA. The difference between their spectral characteristics is readily apparent—the first component (OA) has a stronger blue signal but a weaker green signal than the second component (DA). The ability to differentiate two poorly resolved components on the basis

of their different spectral characteristics is useful in several situations. For example, it can confirm that complex peak shapes are from multiple compounds rather than other separation and sample factors, such as slow lysing of subcellular compartments [8].

Single-cell analysis

The CNS of the pond snail *Lymnaea stagnalis* contains several neurons that have been biochemically characterized, and so has been used to explore the utility of this new instrument for single-cell analysis of neurotransmitters. The pedal ganglia of this CNS has a pair of symmetrical,

Fig. 6 Comparison of representative electropherograms obtained after (a) injection of homogenized commissure tissue from a buccal ganglion of *Aplysia californica*, and (b) whole-cell injection of an RPeD1 cell from *Lymnaea stagnalis*



identified neurons, termed the right and left pedal dorsal 1 (RPeD1 and LPeD1), that contain DA and 5-HT, respectively [31, 32]. RPeD1 is a component of the central pattern-generator network, which controls hypoxia-driven respiration and coordinates sensory motor input from the pneumostome to initiate respiratory rhythm generation [33]. We conducted comparative analysis of the buccal commissure from the CNS of *Aplysia californica* and a single RPeD1 cell, which also contains DA [34]; two of the electropherograms obtained are presented in Fig. 6. Note that although the traces are qualitatively similar, the migration times differ substantially, because large and inconsistent amounts of proteins and undissolved cellular components are injected into the capillary with the analyte of interest. Positive identification of DA based on migration-time alone is therefore problematic.

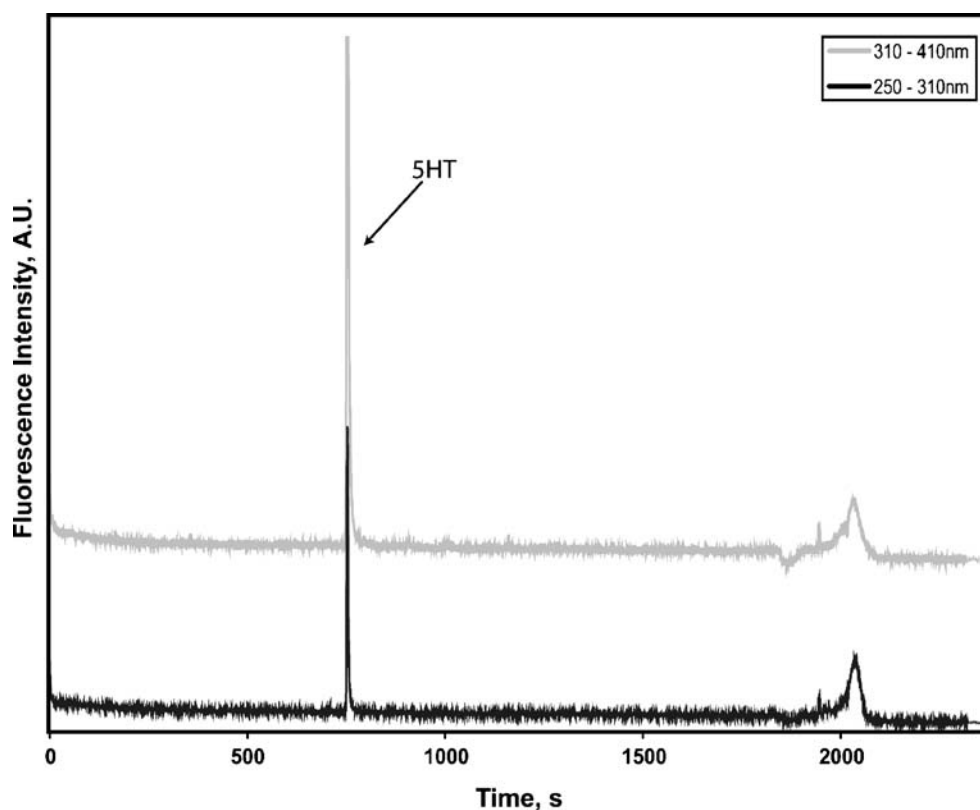
In addition to the qualitative similarities of the single RPeD1 neuron electropherogram to that of dopaminergic tissue, the multichannel ratio for the intense early peak from RPeD1 ($G/B_{\text{average}}=1.727$) enables statistical comparison with ratios calculated using standard DA solutions ($G/B_{\text{average}}=1.746$). Single-factor analysis of variance (ANOVA) indicates that these ratios are indistinguishable at a 95% confidence level ($\alpha=0.05$), with $\nu=4$ and a p -value of 0.31. Thus, the multichannel detector supports the identification of DA in a single RPeD1 neuron. An

electropherogram resulting from the investigation of an isolated LPeD1 cell is provided, for comparison, in Fig. 7; the spectral characteristics of the main peak in this electropherogram are inconsistent with those of DA, but consistent with its identity as 5-HT.

Conclusions

A PMT-based, multichannel detection system with a 224-nm HeAg laser as its excitation source enables sensitive CE-LINF analysis without the complexity and cost associated with CCD-based wavelength-resolved systems. The LODs for neurotransmitters are in the low nanomolar (attomole) range. The instrument can be used to discriminate between different catecholamines and indolamines, and is sensitive enough to detect their presence in single neurons. The sensitivity of the system enables the composition of these cells to be probed while obtaining $S/N>50$ for the transmitters. This implies that smaller neurons (or subcellular compartments) can be analyzed with adequate sensitivity. This will enable experiments on catecholamine signaling to be undertaken that are similar to our single-cell experiments investigating 5-HT signaling [35].

Fig. 7 Electropherogram obtained after whole-cell injection of a serotonergic LPeD1 cell from *Lymnaea stagnalis*. Excitation at 224 nm also enables sensitive detection of indolamines such as 5-HT



Acknowledgements This material is based upon work supported by NIH under award no. DK070285. The authors would like to thank Christine Cecala and Kevin Tucker, University of Illinois at Urbana-Champaign, and Ray Reid, Bill Hug, and Sam Panigrahi from Photon Systems, Inc. We would also like to acknowledge the assistance of the School of Chemical Sciences machine shop, especially Tom Wilson and Bill Knight. The acquisition of *Aplysia californica* was partially supported by the National Resource for Aplysia at the University of Miami under NIH National Center for Research Resources grant RR10294.

References

1. Axelrod J, Saavedra JM (1977) *Nature* 265:501–504
2. Premont RT, Gainetdinov RR, Caron MG (2001) *Proc Natl Acad Sci USA* 98:9474–9475
3. Kennedy RT, Oates MD, Cooper BR, Nickerson B, Jorgenson JW (1989) *Science* 246:57–63
4. Stuart JN, Sweedler JV (2003) *Anal Bioanal Chem* 375:28–29
5. Ahmadzadeh H, Johnson RD, Thompson L, Arriaga EA (2004) *Anal Chem* 76:315–321
6. Chen Y, Arriaga EA (2006) *Anal Chem* 78:820–826
7. Ewing AG, Wallingford RA, Olefirowicz TM (1989) *Anal Chem* 61:292A–303A
8. Kristensen HK, Lau YY, Ewing AG (1994) *J Neurosci Methods* 51:183–188
9. Dovichi NJ, Hu S (2003) *Curr Opin Chem Biol* 7:603–608
10. Olefirowicz TM, Ewing AG (1990) *J Neurosci Methods* 34:11–15
11. Miao H, Rubakhin SS, Sweedler JV (2003) *Anal Bioanal Chem* 377:1007–1013
12. Wallingford RA, Ewing AG (1987) *Anal Chem* 59:1762–1766
13. Cheng YF, Dovichi NJ (1988) *Science* 242:562–564
14. Chang HT, Yeung ES (1995) *Anal Chem* 67:1079–1083
15. Liu CC, Zhang J, Dovichi NJ (2005) *Rapid Commun Mass Spectrom* 19:187–192
16. Sweedler JV, Shear JB, Fishman HA, Zare RN, Scheller RH (1992) Analysis of neuropeptides using capillary zone electrophoresis with multichannel fluorescence detection. *Proceedings of SPIE-The International Society for Optical Engineering*; p. 37–46
17. Timperman AT, Khatib K, Sweedler JV (1995) *Anal Chem* 67:139–144
18. Shippy SA, Jankowski JA, Sweedler JV (1995) *Anal Chim Acta* 307:163–171
19. Timperman AT, Sweedler JV (1996) *Analyst* 121:45R–52R
20. Okerber E, Shear JB (2001) *Anal Biochem* 292:311–313
21. Wise DD, Shear JB (2006) *J Chromatogr A* 1111:153–158
22. Karger AE, Harris JM, Gesteland RF (1991) *Nucleic Acids Res* 19:4955–4962
23. Gilman SD, Ewing AG (1995) *Anal Chem* 67:58–64
24. Oldenburg KE, Xi X, Sweedler JV (1997) *J Chromatogr A* 788:173–183
25. Thongkhaio-On K, Kottegoda S, Pulido JS, Shippy SA (2004) *Electrophoresis* 25:2978–2984
26. Hu S, Michels DA, Fazal MA, Ratisoontorn C, Cunningham ML, Dovichi NJ (2004) *Anal Chem* 76:4044–4049
27. Fuller RR, Moroz LL, Gillette R, Sweedler JV (1998) *Neuron* 20:173–181
28. Zhang X, Sweedler JV (2001) *Anal Chem* 73:5620–5624
29. Park YH, Zhang X, Rubakhin SS, Sweedler JV (1999) *Anal Chem* 71:4997–5002
30. Shear JB (1999) *Anal Chem* 71:598A–605A
31. Cottrell GA, Abernethy KB, Barrand MA (1979) *Neuroscience* 4:685–687
32. Audesirk G (1985) *Comp Biochem Physiol A* 81:359–365
33. Haque Z, Lee TKM, Inoue T, Luk C, Hasan SU, Lukowiak K, Syed NI (2006) *Eur J Neurosci* 23:94–104
34. Díaz-Ríos M, Oyola E, Miller MW (2002) *J Comp Neurol* 445:29–46
35. Stuart JN, Zhang X, Jakubowski JA, Romanova EV, Sweedler JV (2003) *J Neurochem* 84:1358–1366